Electronic Supplementary Material (ESI) for Inorganic Chemistry Frontiers.

Efficient Ammonia Synthesis over a Core-shell Ru/CeO_2 Catalyst with Tunable CeO_2 Size: DFT Calculation and XAS Spectroscopy Studies

Xiuyun Wang[a], Xuanbei Peng[a], Yongfan Zhang[b], Jun Ni[a] and Lilong Jiang[a]*

[a]*National Engineering Research Center of Chemical Fertilizer Catalyst, Fuzhou University, Fuzhou, Fujian 350002, China.*

[b]*College of Chemistry, Fuzhou University, Fuzhou, Fujian, 350116, China.*

Corresponding author E-mail: jllfzu@sina.cn, jll@fzu.edu.cn.

Figure S1 SEM images of (A) CSs-7, (E) CSs-9, and (I) CSs-11; (B) CSs-7@CeO_2, (F) CSs-9@CeO_2 and (J) CSs-11@CeO_2; (C) CSs-7@Ru-CeO_2, (G) CSs-9@Ru-CeO_2 and (K) CSs-11@Ru-CeO_2; (D) Ru@CeO_2-7; (H) Ru@CeO_2-9 and (L) Ru@CeO_2-11 of core−shell structure. (Page 2)

Figure S2 TEM images of (A) Ru@CeO_2-7, (B) Ru@CeO_2-9 and (C) Ru@CeO_2-11. Particle distribution of Ru nanoparticles over (A) Ru@CeO_2-7, (B) Ru@CeO_2-9 and (C) Ru@CeO_2-11.

Figure S3 Raman spectra of (A) CeO_2 supports and (B) Ru@CeO_2 catalysts after activity test. (Page 2)

Figure S4 H_2-TPR profiles of (A) CeO_2 supports and (B) Ru@CeO_2 catalysts. (Page 3)

Figure S5 SEM images of Ru@CeO_2-9 after activity and thermal stability test of 72 h. (Page3)

Figure S6 XPS spectra: (A) Ce3d of CeO_2 supports, (B) Ru3d and (C) Ru3p of H_2-reduced Ru@CeO_2 catalysts. (Page4)

Figure S7 in situ DRIFTS experiment of Ru@CeO_2-9 at 400 ^oC with different time (test condition: 10%CO+Ar)

Mass Transfer Calculation for ammonia synthesis over the Ru@CeO_2-9 catalyst (Page5)

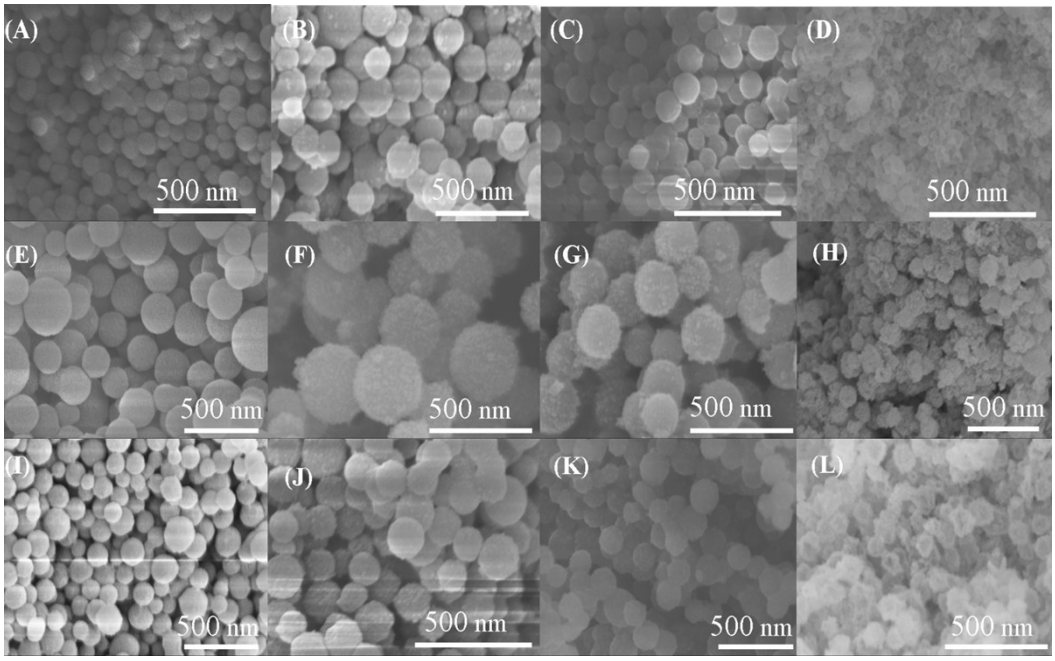

Figure S1 SEM images of (A) CSs-7, (E) CSs-9, and (I) CSs-11; (B) CSs-7@CeO_2, (F) CSs-9@CeO_2 and (J) CSs-11@CeO_2; (C) CSs-7@Ru-CeO_2, (G) CSs-9@Ru-CeO_2 and (K) CSs-11@Ru-CeO_2; (D) Ru@CeO_2-7; (H) Ru@CeO_2-9 and (L) Ru@CeO_2-11 of core−shell structure.

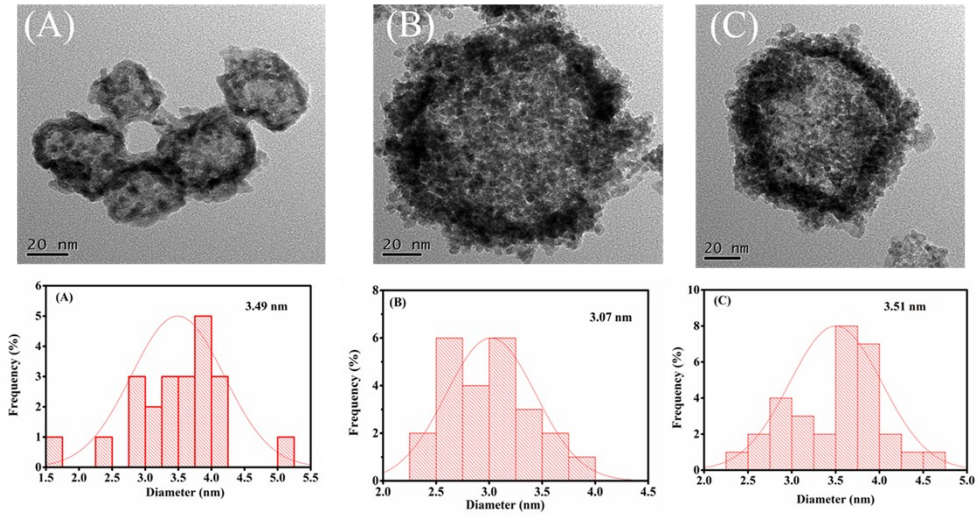

Figure S2 TEM images of (A) Ru@CeO_2-7, (B) Ru@CeO_2-9 and (C) Ru@CeO_2-11. Particle distribution of Ru nanoparticles over (A) Ru@CeO_2-7, (B) Ru@CeO_2-9 and (C) Ru@CeO_2-11.

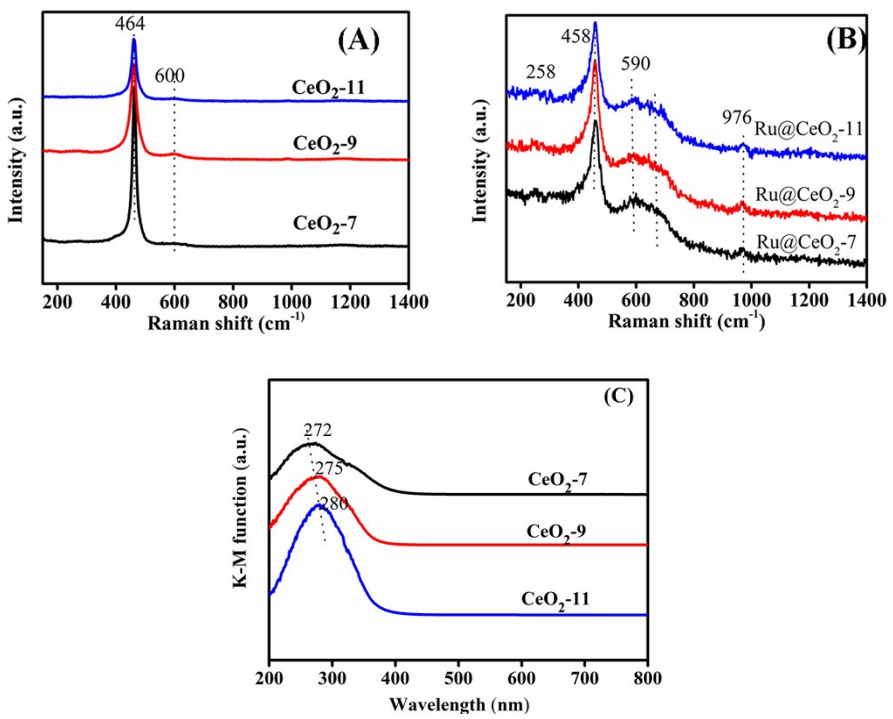

Figure S3 Raman spectra of (A) CeO_2 supports; (B) Ru@CeO_2 catalysts after activity test and (C) Uv-vis spectra of CeO_2 supports.

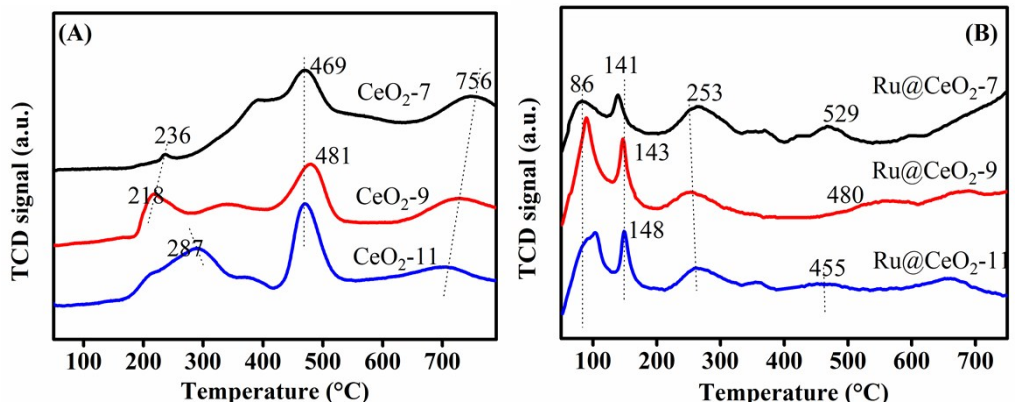

Figure S4 H_2-TPR profiles of (A) CeO_2 supports and (B) Ru@CeO_2 catalysts.

H_2-TPR profiles of CeO_2 and Ru@CeO_2 are shown in Figure 7. For pure CeO_2-7, the peaks located at 236 °C and 469 °C are related to the reduction of surface oxygen, while the peak above 700 °C is associated with the reduction of lattice oxygen species. Unlike CeO_2-7, CeO_2-9 and CeO_2-11 show low-temperature reduction peaks at 218 and 209 °C, indicating that the surface oxygen species on CeO_2-9 and CeO_2-11 are more easily reduced. For all the Ru@CeO_2 catalysts generated using the CeO_2

supports, RuO_2 can be reduced below 150 °C. It is deduced that with the weakening of Ce–O bond by the strongly bound Ru species, the reduction of surface oxygen species on CeO_2-9 and CeO_2-11 becomes more facile. Furthermore, the strong Ce–O–Ru bonding causes electron transfer from Ru to the CeO_2 support, thus forming $Ru^{\delta+}$. We roughly estimated the relative number of $Ru^{\delta+}$ and Ce–O–Ru bonds based on the area of the corresponding reduction peaks. It is observed that the relative number of Ru–O–Ce and $Ru^{\delta+}$ follows the order of Ru@CeO_2-9 > Ru@CeO_2-11 > Ru@CeO_2-7.

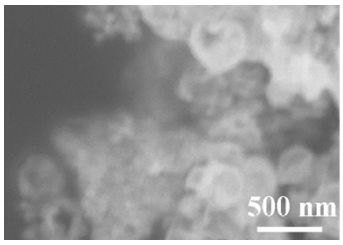

Figure S5 SEM images of Ru@CeO_2-9 after activity and thermal stability test of 72 h.

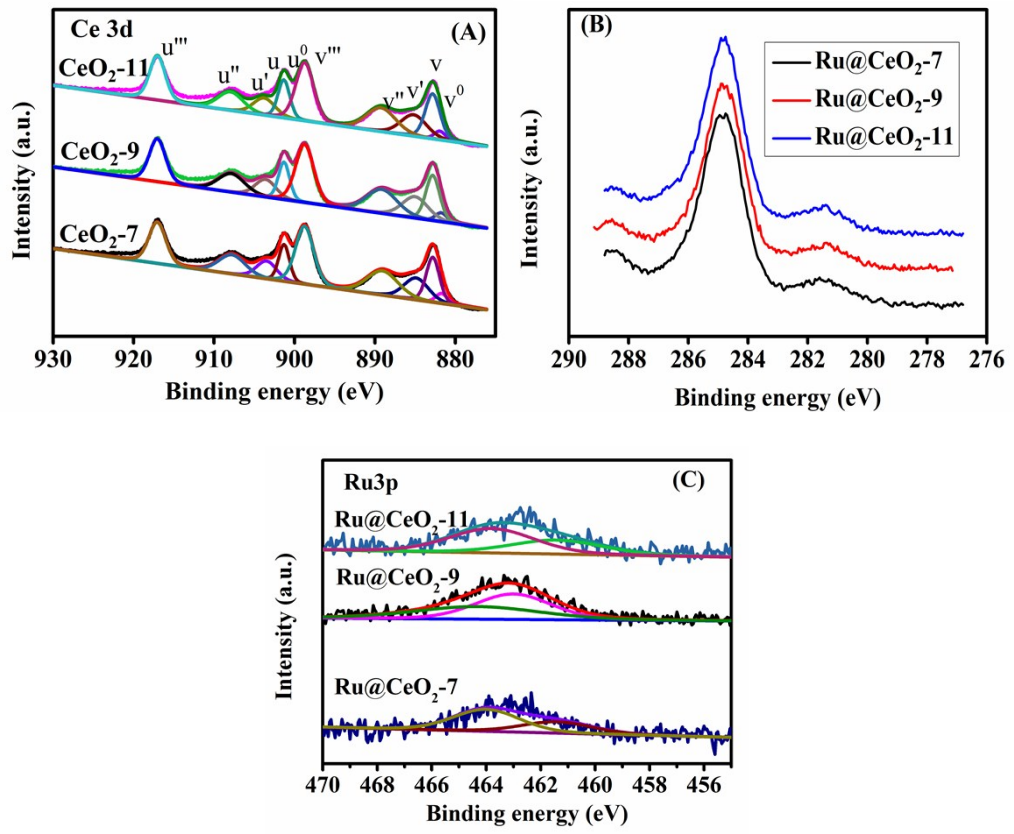

Figure S6 XPS spectra: (A) Ce3d of CeO_2 supports, (B) Ru3d and (C) Ru3p of H_2-

reduced Ru@CeO_2 catalysts.

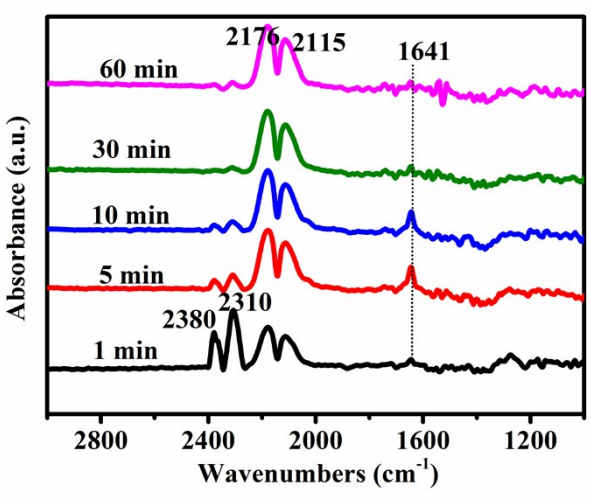

Figure S7 in situ DRIFTS experiment of Ru@CeO_2-9 at 400 °C with different time (test condition: 10%CO+Ar)

Mass Transfer Calculation for ammonia synthesis over the Ru@CeO_2-9 catalyst

Mears Criterion for External Diffusion (Fogler, p841; Mears, 1971)

If $\frac{-r_A' \rho_b R n}{k_c C_{Ab}} < 0.15$, the external mass transfer effects can be neglected.

$-r_A'$ = reaction rate of nitrogen, kmol/(kg·cat·s)

n = reaction order with respect to nitrogen gas.

R = average radius of catalyst particles, m

ρ_b = bulk density of catalyst bed, kg/m^3

C_{Ab} = bulk gas concentration of nitrogen, kmol/m^3

k_c = mass transfer coefficient, m/s

$\frac{-r_A' \rho_b R n}{k_c C_{Ab}}$ =[2x 10^{-7} kmol-N_2/(kg·cat·s] [910 kg/m^3][2.5 x 10^{-4} m][1]/([1.7m/s]*[0.04 kmol/m^3])=**0.67x10^{-7} <0.15 {Mears for External Diffusion}**

Weisz-Prater Criterion for Internal Diffusion (Fogler, p839)

If $C_{WP} = \frac{-r'_{A(obs)} \rho_c R^2}{D_e C_{As}} < 1$, the internal mass transfer effects can be neglected.

$-r'_{A(obs)}$ = reaction rate of nitrogen, kmol/(kg·cat·s)

ρ_c is solid catalyst density, kg/m^3

R = average radius of catalyst particles, m

ρ_b = bulk density of catalyst bed, kg/m^3

C_{Ab} = bulk gas concentration of nitrogen, kmol/m^3

D_e = effective gas-phase diffusivity, m^2/s **[Fogler, p815]**

C_{As} = gas concentration of A at the catalyst surface, kmol-A/m^3

$C_{WP} = \frac{-r'_{A(obs)} \rho_c R^2}{D_e C_{As}}$ = [2 x 10^{-7} kmol-N_2/(kg·cat·s)] [2.8*10^3 kg-cat/m^3] *[2.5 x 10^{-4} m]^2/([3.3 x 10^{-6} m^2/s]* [0.04 kmol-N_2/m^3]) = **2.65x 10^{-4} < 1**

{Weisz-Prater Criterion for Internal Diffusion}